The Protective Effect of Diphenoxylate Drug on API X120 Carbon Steel Corrosion in 15% Hydrochloric Acid Environment

Lebe A. Nnanna[1], Nkem B. Iroha[2,*]

[1]Department of Physics, Michael Okpara University of Agriculture, Umudike, Abia State, Nigeria
[2]Electrochemistry and Material Science Unit, Department of Chemistry, Federal University Otuoke, P.M.B. 126 Yenagoa, Bayelsa State, Nigeria

*Corresponding author: E-mail: nkemib@yahoo.com

DOI: 10.5185/amlett.2020.051511

The inhibiting effect of diphenoxylate drug (DD) on API X120 carbon steel corrosion in 15% HCl solution was investigated using chemical, electrochemical and surface morphological studies. The inhibition efficiency of the studied drug increases with increase in its concentrations, giving a maximum inhibition efficiency of 95.28%, at the optimum concentration of 400 ppm. The effect of temperature revealed that the inhibition efficiency of DD decreases with temperature rise. The adsorption of DD obeyed the Langmuir isotherm and indicated predominantly physical adsorption mechanism. The electrochemical impedance spectroscopy (EIS) analysis affirmed the adsorption of the inhibitor on the X120 steel surface. Potentiodynamic polarization (PDP) study indicated that the tested drug acted as mixed type inhibitor with little anodic dominance. The result of scanning electron microscopy (SEM) and energy-dispersive X-ray (EDX) spectroscopy supported the formation of adsorbed inhibitor film on the X120 steel surface.

Introduction

Corrosion of carbon steel in acid environments is a huge problem in many industries, particularly in the oil and gas industry. Acid solutions are frequently used in several industrial processes such as the petrochemical processes, oil well acidification, acid pickling and acidic cleaning [**1-3**]. One important method of protecting carbon steel from corrosion is by the use of corrosion inhibitors. Scientists have unanimously agreed that this protection is usually attributed to the adsorption of inhibitors on the metal surface. The adsorption of these corrosion inhibitors is determined by different factors like; presence of functional group such as C=O, -N=N-, R-OH etc., the electronic structure of the inhibiting molecules, aromaticity, steric factor, molecular weight of the inhibitor molecule and electron density at donor site [**4,5**]. Recently, researchers have synthesized organic compounds and found them to be good corrosion inhibitors for steel in hydrochloric acid [**6,7**].

Many synthetic organic and inorganic inhibitors offer good protection against metal corrosion but majority of these inhibitors are hazardous to both the environment and human beings, which restricts their application. Mostly, green organic corrosion inhibitors are more eco-friendly than inorganic inhibitors [**8**]. Some researchers have considered the use of drugs as corrosion inhibitors for steel in different acids [**9-11**] because of their environmental friendly nature which gives them advantage over the use of inorganic and some organic inhibitors.

In our previous work [**12**], the anticorrosion behavior of cefepime, a fourth generation cephalosporin antibiotic, in controlling X80 pipeline steel corrosion in 1.0 M HCl solution was studied by weight loss and electrochemical methods. To complement this study, the protective effects of diphenoxylate drug on API X120 carbon steel corrosion in 15% hydrochloric acid environment is being investigated using gravimetric, electrochemical and surface morphological studies. Diphenoxylate is a centrally active opioid drug of the phenylpiperidine series that is used in a combination drug with atropine for the treatment of diarrhea. The chemical name of diphenoxylate is ethyl 1-(3-cyano-3,3-diphenylpropyl)-4-phenylpiperidine-4-carboxylate and its chemical formula is $C_{30}H_{32}N_2O_2$ with molecular mass of 452.587 g/mol. Diphenoxylate has 2N and 2O active centers which favour the interaction of the drug with the metal. To the best of our knowledge, diphenoxylate has not been used as an inhibitor for the corrosion of any metal in acid environment. The chemical structure of the diphenoxylate is shown in **Fig. 1**.

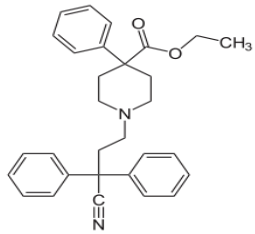

Fig. 1. Structure of Diphenoxylate molecule.

Experimental

Materials and test solution

API X120 Carbon steel specimen containing C = 0.129%, Si = 0.101%, Mn = 0.541%, Ni = 0.017%, Cr = 0.039%, Mo = 0.0013%, Cu = 0.015%, V = 0.025% and the balance Fe were press cut into coupons with different dimensions based on the method of experiment. The surface of the coupons were polished using SiC papers of 400 - 800 grades, washed under running water, degreased with acetone, dried in air and kept in a desiccator prior to use in corrosion studies. Precise weights of the coupons were taken and recorded, using Ohaus Adventurer digital analytical balance. All reagents and chemicals used were of analytical grade. The blank test solution contained 15% HCL.

Diphenoxylate drug (DD) marketed under the brand name Lomotil was used as the corrosion inhibitor. The drug was procured and used without further purification. Different amounts of DD were dissolved in 15% HCL solution to prepare the desired inhibitor concentrations in parts per million (ppm).

Gravimetric method

The X120 Carbon steel specimens with dimension of 1 × 4 × 1 cm were used for the gravimetric experiments. Previously weighed coupons were placed in a 250 ml beaker, which contained 100 ml of test solutions of 15% HCl used for the blank experiment and different concentrations (100 – 400 ppm) of Diphenoxylate drug (DD) maintained at 30, 40, 50, and 60°C in a thermostated water bath. Each coupon was retrieved from the test solution after 5 h, washed with double distilled water, dried and reweighed to determine the weight loss of the coupon. Quadruplet experiments were run in each case and the average values recorded. The corrosion rates (CR), were calculated using the equation:

$$CR = \frac{\Delta W}{A.t} \quad (1)$$

Here, ΔW is the weight loss of X120 steel coupon, A is the total area of the steel coupon and t is immersion time (5 h). With the calculated corrosion rate, the inhibition efficiency η_{WL}% was calculated as follows:

$$\eta_{WL}\% = 100\left[\frac{CR^{bla} - CR^{inh}}{CR^{bla}}\right]$$

Surface coverage (θ) was calculated from the following equations:

$$\theta = \frac{\eta_{WL}\%}{100} \quad (3)$$

where CR^{bla} and CR^{inh} are the corrosion rates of the X120 carbon steel specimen in the absence and presence DD inhibitor respectively.

Electrochemical experiments

The electrochemical (potentiodynamic polarization (PDP) and electrochemical impedance spectroscopy (EIS)) experiments were carried out using Gamry Potentiostat/Galvanostat (Model G-300) connected to a personal computer with EIS software Gamry Instruments Inc., USA. The conventional three electrode cell of 250 mL capacity was used. The working electrode was X120 steel while a saturated calomel electrode (SCE) was the reference electrode. Platinum foil (1 cm^2) was the counter electrode. Echem Analyst 6.0 software package was used to analyze the electrochemical experiments. All electrochemical tests were run after immersion of X120 steel for 1h to attain stable open circuit potential in the 15% HCl with and without addition of the inhibitor. The EIS measurement was performed in the frequency range of 100 kHz to 10 mHz, with amplitude of 10 mV peak-to-peak, at open circuit potential (OCP). PDP measurement was carried out by shifting the electrode potential from -250 mV to +250 mV versus OCP at a scan rate of 1 mV/s. All electrochemical experiments were performed at 30 °C temperature.

Surface analysis

The X120 steel specimens with polished and cleaned surfaces were immersed in 1 M HCl solution in the absence and presence of 2.5 g/L concentration of DD at 30 °C. The samples were retrieved after 6 h of immersion, rinsed with double distilled water, degreased in acetone and dried in air. Scanning electron microscopy (SEM) studies were performed by using a Quanta 250F instrument model at an accelerating voltage of 5 kV and 1.5k magnification. Chemical composition of the X120 steel surface was recorded by an energy-dispersive X-ray (EDX) spectroscopy detector.

Results and discussion

Gravimetric measurements

Effect of inhibitor concentration

The effect of Diphenoxylate drug (DD) concentration on the corrosion rate (CR) of X120 steel in 15% HCl solution and the inhibition efficiency (η_{WL}%) are shown in **Fig. 2(a)**. It is obvious that as the DD concentration increases the corrosion rate decreases while the inhibition efficiency increases. This indicates that the corrosion inhibition of DD is strengthened by the drug concentration. This tendency could be as a result of the facts that increase in concentration of corrosion inhibitors increases the surface coverage which leads to effective separation of the X120 steel from the corrosive medium by the formation of a protective adsorbed film on its surface.

Effect of temperature

Fig. 2(b) shows the temperature dependence of corrosion rate of X120 steel and the inhibition efficiency of DD. Corrosion rate was observed to increase as the temperature

increased from 30ºC to 60ºC. This observation shows that the corrosion of X120 steel is in agreement with chemical reaction general principle which says that the rate of a chemical reaction increases with increase in temperature. On the other hand, the inhibition efficiency followed a reverse trend, decreasing with rise in temperature. This is perhaps, due to desorption of the molecules of the inhibitor from the X120 steel surface at higher temperature.

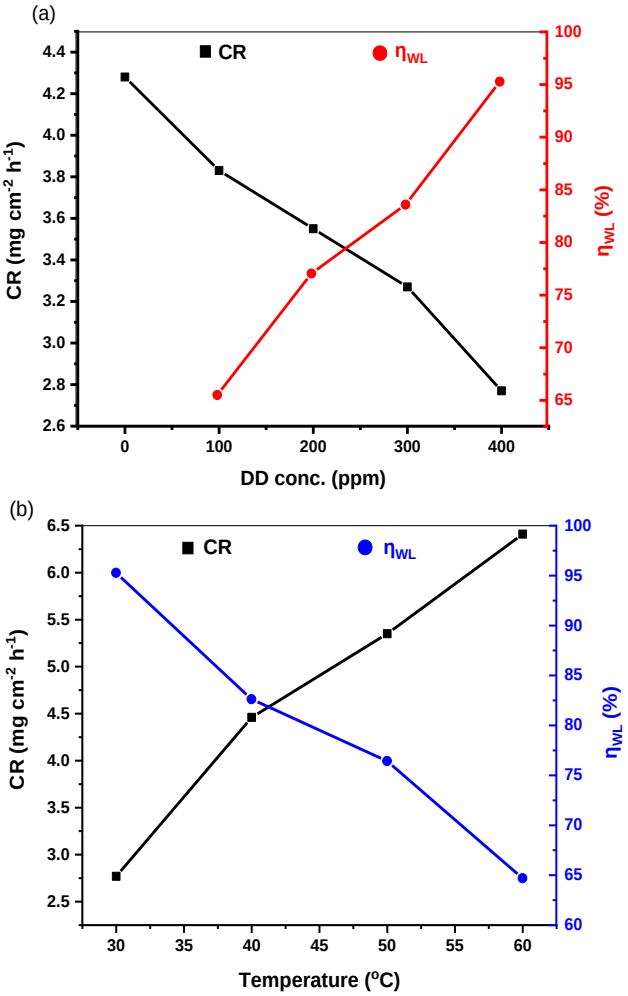

Fig. 2. (a) Variation of CR and η_{WL}% with inhibitor concentration at 30ºC and (b) Variation of CR and η_{WL}% with solution temperature (30 - 60ºC) at optimum concentration of DD.

The effect of temperature on the corrosion inhibition of X120 steel in the absence and presence of different concentration of DD was further investigated using the Arrhenius and Eyring transition state equations, represented as shown in equations 4 and 5 respectively [**13,14**]

$$CR = A\exp\left(-\frac{E_a}{RT}\right) \quad (4)$$

$$CR = \left(\frac{RT}{Nh}\right)\exp\left(\frac{\Delta S^O}{R}\right)\exp\left(\frac{-\Delta H^O}{RT}\right) \quad (5)$$

where CR represents corrosion rate of the X120 steel, A is the pre-exponential factor, E_a is the apparent activation energy, R is the gas constant, T is the absolute temperature, N is Avogadro's number and h is Plank's constant, while ΔS^0 and ΔH^0 are the entropy and the enthalpy of activation respectively. Arrhenius plots of log CR versus 1000/T gives a straight line, as revealed by **Fig. 3(a)** and the activation energy E_a was calculated from the slope of the linear plots and listed in **Table 1**. Eyring transition state plots of log (CR/T) versus (1000/T) gives a straight line with a slope of ($-\Delta H^0/2.303R$) and an intercept of $\log(R/Nh)+\Delta S^0/2.303R$, as depicted in **Fig. 3(b)** and the values of ΔH^0 and ΔS^0 were calculated from slope and intercept respectively and listed in **Table 1**.

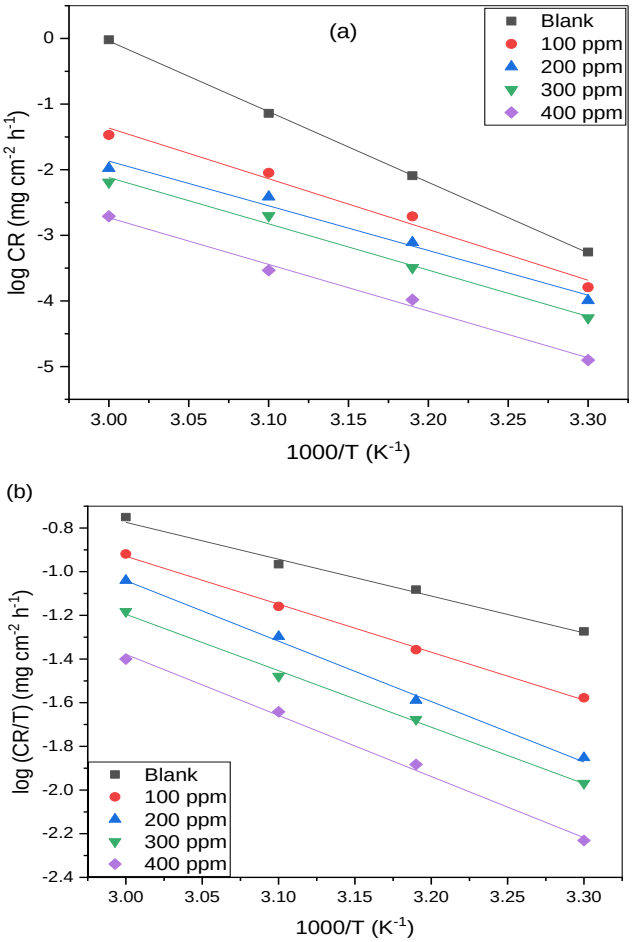

Fig. 3. (a) Arrhenius plots of log CR vs. 1000/T and (b) Transition state plots for the corrosion of X120 steel in 15% HCl solution without and with different concentrations of DD.

Table 1. Calculated values of activation parameters for Q235 mild steel corrosion in 0.5 M H_2SO_4 in the absence and presence of MAE

Conc. (ppm)	E_a (kJ/mol)	ΔH^0 (kJ/mol)	ΔS^0 (J/mol/K)
Blank	58.84	37.65	-161.34
100	65.37	41.50	-154.69
200	69.16	44.91	-149.31
300	74.32	49.62	-140.84
400	77.90	52.44	-132.86

It is observed from **Table 1** that for the 15% HCl blank solution the E_a value is 58.84 kJ/mol. This value is found to increase in the presence of DD which reveals the retardation of the corrosion reaction in the inhibited solutions. Reports [**15-17**] have also shown that higher value of E_a in the presence of inhibitors compared to the blank acid solution is attributed to physical adsorption while the reverse is taken to mean chemisorption mechanism. The positive sign of ΔH^0 indicates the endothermic nature of the activated step of the corrosion process [**18**]. The values of ΔS^0 are seen to be negative both in the uninhibited and inhibited solutions which indicate that the activated complex in the rate determining step represents association instead of dissociation [**19**].

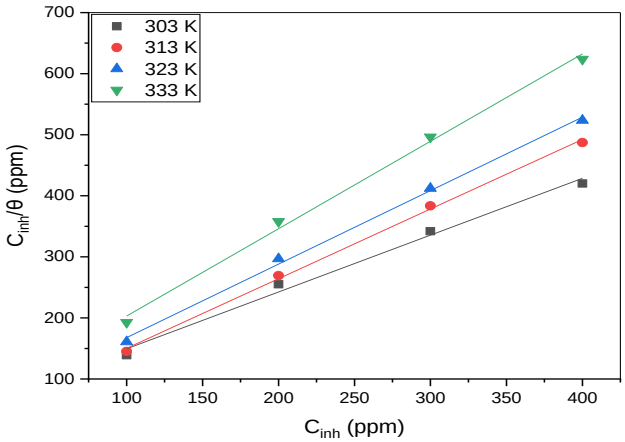

Fig. 4. Langmuir isotherm plots for X120 steel in 15% HCl with different concentrations of DD at 303 – 333 K.

Adsorption isotherms

The adsorption isotherms provide basic information on the interaction between inhibitor molecules and the metal surfaces. The degree of surface coverage (θ) obtained from gravimetric measurements at different DD concentrations in 15% HCl solution was tested with Langmuir adsorption isotherm according to the relation:

$$\frac{C_{inh}}{\theta} = \frac{1}{K_{ads}} + C_{inh} \quad (6)$$

where K_{ads} is the adsorption equilibrium constant and C_{inh} represents the inhibitor concentration. A linear graph was obtained by plotting C_{inh}/θ versus C_{inh}. The values of K_{ads} were deduced from the intercepts of the plots (**Fig. 4**) and listed in **Table 2**, with other values of Langmuir adsorption parameters obtained from the plots. The results indicate that the R^2 values and the slopes for the plots are very close to unity, which shows that the adsorption of DD on the X120 steel follows Langmuir isotherm. K_{ads} is known to represent the strength of adsorption or desorption between the adsorbent (metal surface) and the adsorbate (inhibitor molecule) with higher values of K_{ads} corresponding to better adsorption. **Table 2** shows that K_{ads} decreased with temperature rise, an indication that DD molecules were strongly adsorbed onto the X120 steel surface at lower temperature, which appears to desorb at higher temperature. The adsorption equilibrium constant (K_{ads}) is related to the standard free energy of adsorption (ΔG^0_{ads}) according to the following equation:

$$\Delta G^0_{ads} = -RT\ln(55.5K_{ads}) \quad (7)$$

where R is the universal constant, T is the absolute temperature and the value 55.5 is the molar concentration of water in solution. The calculated values of ΔG^0_{ads} are also listed in **Table 2**. The ΔG^0_{ads} values are all negative which indicates spontaneity of the processes of adsorption and stability of the adsorbed film on the surface of the X120 steel.

Table 2. Adsorption parameters for DD obtained from Langmuir adsorption isotherm at different temperatures.

Temp. (K)	R^2	Slope	K_{ads} (ppm^{-1})	- ΔG_{ads} (kJ/mol)
303	0.9912	0.9307	0.0091	31.11
313	0.9984	1.1403	0.0057	30.95
323	0.9977	1.2036	0.0051	31.66
333	0.9964	1.4315	0.0048	32.39

Literature has reported that the value of ΔG^0_{ads} around −20 kJ/mol or less negative indicates physisorption process which has to do with electrostatic interaction between charged metal surface and charged molecules in the solution, while those around −40 kJ/mol or more is understood to be chemisorption involving charge transfer or sharing between the metal surface and organic inhibitor molecules [**20**]. The ΔG^0_{ads} values as shown in **Table 2** are in the range 30.95 and 32.39 kJ/mol which means the values are in-between the two thresholds that correspond to chemisorption and physisorption mechanisms. Thus, it can be deduced that the adsorption of DD on API 5L X120 steel surface may involve physisorption and chemisorption processes but predominantly physisorption [**21, 22**].

Electrochemical studies

Polarization study

The Tafel polarization curves for X120 steel in 15% HCl in the absence and presence of diphenoxylate drugs (DD) at different concentrations are shown in **Fig. 5**. The polarization parameters like, corrosion current density (i_{corr}), corrosion potential (E_{corr}), anodic (β_a) and cathodic (β_c) Tafel slopes, derived by extrapolation of the linear component of the Tafel plots are listed in **Table 3**. The results revealed that in the presence of DD inhibitor, i_{corr} for cathodic and anodic curves is displaced towards the lower current parts as compared to the i_{corr} of the blank 15% HCl solution. The i_{corr} values were found to decrease with increase in inhibitor concentration. This indicates that the DD inhibitor is adsorbed on the X120 steel surface, retarding both anodic (X120 steel dissolution) and cathodic (hydrogen evolution) reactions [**23**]. In addition, the shapes of the Tafel curves in the absence and presence of the inhibitor are similar, indicating that DD inhibits the X120 steel corrosion by formation of protective film on the surface without changing the corrosion mechanism [**24, 25**].

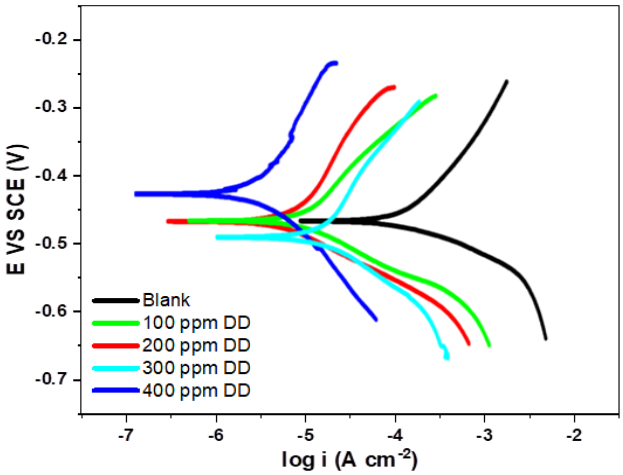

Fig. 5. Tafel polarization curves of X120 steel in 15% HCl in the absence and presence of DD.

Table 3. Polarization parameters for X120 steel corrosion in 15% HCl without and with various concentrations of DD.

DD Conc. (ppm)	E_{corr} (mV/SCE)	β_c (mV/dec)	β_a (mV/dec)	i_{corr} (mA/cm^2)	η_{PDP} (%)
0	-521	283.5	105.7	1358.5	-
100	-509	310.9	143.8	461.6	66.0
200	-492	300.2	162.8	385.2	71.6
300	-483	321.4	174.1	236.7	82.6
400	-479	339..0	188.5	108.3	92.0

On proper examination of results shown in **Table 3**, it can be seen that the displacement in E_{corr} values is less than 85 mV and shifts toward the less negative side with increase in the concentration of the inhibitor. According to reports in literature [**26-28**], the displacement in the E_{corr} values less than 85 mV indicates that the inhibitor acts as a mixed type inhibitor but if greater than 85 mV, the inhibitor acts as an anodic or cathodic type inhibitor. The present study reports that the maximum displacement in the E_{corr} value is 42 mV, which implies that DD inhibitor is a mixed-type with little anodic dominance. It can also be seen from **Table 3**, that in the presence of DD, the values of β_a are slightly more affected as compared to the values of β_c, which supports the fact that the DD inhibitor acts as a predominantly anodic type inhibitor.

The inhibition efficiency (η_{PDP}) of DD listed in **Table 3** was calculated from the i_{corr} value using the following equation:

$$\eta_{PDP}(\%) = \left(1 - \frac{i_{corr}^{I}}{i_{corr}^{B}}\right)100 \qquad (8)$$

where i_{corr}^{B} and i_{corr}^{I} are the corrosion current densities in the absence and presence of DD inhibitor. The calculated values reveal that η_{PDP} increased with DD concentration, which is in good agreement with the results obtained from the gravimetric study.

Electrochemical impedance spectroscopy study

The impedance study was carried out at an invariant temperature of 30°C, and the effects of various concentrations of diphenoxylate drugs (DD) in 15% HCl solution were determined. Nyquist plots of X120 steel in the absence and presence of DD are depicted in **Fig. 6a**. The diagram shows a depressed semicircle with a capacitive loop in the high frequency (HF) region and a well-defined small inductive loop at low frequency (LF). The presence of semicircular capacitive loop at HF is attributed to the electric double layer capacitance and the time constant of charge transfer [**29,30**]. The inductive loop at LF may be attributed to the relaxation of adsorbed species on the steel surface [**31,32].** It could also be observed from the figures that the Nyquist curves have similar shape with and without DD inhibitor, suggesting that the addictive inhibits X120 steel corrosion without affecting the reaction mechanism. The depressed nature of the semicircles in the Nyquist plots has been attributed to the inhomogeneities and roughness of the working electrode. [**33**]. It is obvious from **Fig. 6a** that the diameter of the semicircle increases with the increase of DD concentration in 15% HCl environment. This observed increase in diameter indicates the increase in corrosion protective ability of DD because of the adsorption of the inhibitor on the steel surface [**34, 35**].

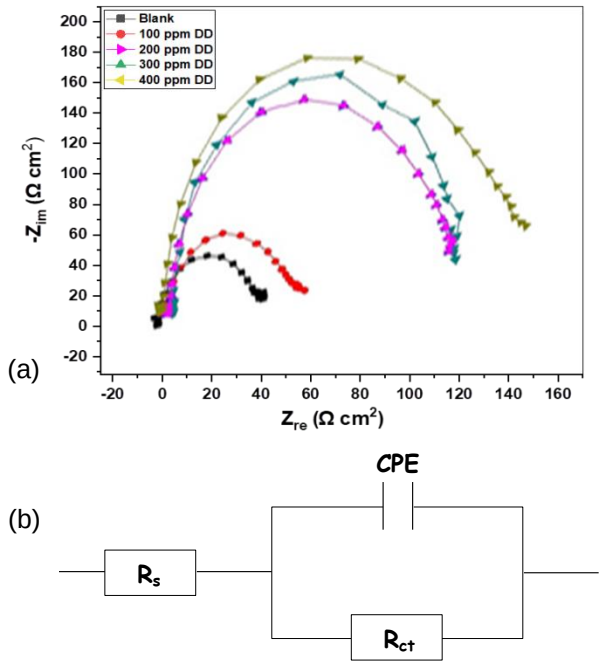

Fig. 6. (a) Nyquist plots of X120 steel in 15% HCl without and with different concentrations of DD at 30°C, (b) Equivalent circuit model used to analyze EIS data.

The EIS data of the Nyquist plots were analyzed using the equivalent circuit model depicted in **Fig. 6b**. In the circuit R_s is the solution resistance, R_{ct} is the charge transfer resistance and CPE is a constant phase element which represents the double-layer capacitance (C_{dl}). The C_{dl} is replaced with a CPE, which is defined by the values of its exponent (n) and its magnitude (Y_0) to compensate for the steel inhomogeneous surface and derive better impedance simulation. The impedance of CPE is defined as [**36**]:

$$Z_{CPE} = \frac{1}{Y_0 (j\omega)^n} \quad (9)$$

where $j = (-1)^{½}$ is the imaginary unit and ω is the angular frequency rad s^{-1} ($\omega = 2\pi f$). For an ideal capacitance the CPE exponent, n = 1 and between the range $0<n\leq1$ in the case of deviation [**37**]. The double-layer capacitance (C_{dl}) values were calculated from the following expression [**38**]:

$$C_{dl} = Y_0^{\frac{1}{n}} R_{ct}^{\frac{1}{n}-1} \quad (10)$$

The fitted EIS parameters using the equivalent circuits are computed and listed in **Table 4**. The inhibition efficiency (η_{EIS}) was calculated by:

$$\eta_{EIS}(\%) = \frac{R_{ct(inh)} - R_{ct(bla)}}{R_{ct(inh)}} \times 100 \quad (11)$$

where $R_{ct(bla)}$ is the charge transfer resistance of the blank, and $R_{ct(inh)}$ is the charge transfer resistance of the inhibited solution. The calculated η_{EIS} is also listed in **Table 4**.

Table 4. EIS parameters obtained from Nyquist plots for X120 steel in 15% HCl without and with different concentrations of DD.

DD Conc. (ppm)	R_s (Ω cm^2)	R_{ct} (Ω cm^2)	Y_o ($\mu\Omega^{-1}s^2cm^{-2}$)	C_{dl} (μFcm^{-2})	n	η_{EIS} (%)
0	1.592	58.4	351.9	453.8	0.919	
100	1.661	154.7	338.2	118.4	0.910	62.2
200	1.794	246.2	341.6	96.1	0.873	76.3
300	1.737	298.9	326.4	78.2	0.908	80.5
400	1.829	590.5	317.5	58.3	0.911	90.1

As seen from the data listed in **Table 4**, it is obvious that the R_{ct} values for the DD inhibited solutions increases whereas the C_{dl} values decreases with increase in the concentration of the inhibitor. This observation is suggestive of the adsorption of the inhibitor molecules on the X120 steel surface, which forms a protective layer at the steel-acid interface. The values of n range from 0.873 to 0.919, which is close to unity, indicating that the CPE relates with the capacitance and the corrosion mechanism of X120 steel is controlled by charge transfer process [**39, 40**]. The increase of R_{ct} values with increasing DD concentration implies that the corrosion process is mainly controlled by the charge transfer process. Also, the decrease in the values of C_{dl} for the inhibited solutions is attributed to decrease in local dielectric constant and/or an increase in the electrical double layer thickness, which verifies that the studied drug inhibit X120 steel corrosion by adsorption at the metal/solution interface thereby reducing the number of available active sites for the corrosion reaction [**41,42**]. The corrosion inhibition efficiency (η_{EIS}) increases with increase in inhibitor concentration. The values of the inhibition efficiency obtained from the EIS study are in good agreement with those obtained from the gravimetric and polarization studies.

Surface morphology studies

The SEM micrographs with the corresponding EDX Spectra for clean polished X120 steel and in absence and presence of diphenoxylate drugs are shown in **Fig. 7(a-c)**. **Fig. 7a(i)** shows the SEM image of the steel surface before immersion in the 15% HCl solution. It is obvious from the figure that the metal surface is relatively smooth. **Fig. 7b(iii)** represents the SEM image of X120 steel dipped in 15% HCl solution in the absence of DD which is highly corroded with clear cracks, due to attack of the acid on the steel. However, in the presence of DD (**Fig. 7c(v)**), the surface morphology of the X120 steel is improved remarkably with the surface becoming smoother. The observation supports the fact that X120 steel is being protected by the adsorption of a thin film of the DD molecules on the metal surface, thereby diminishing the corrosion process.

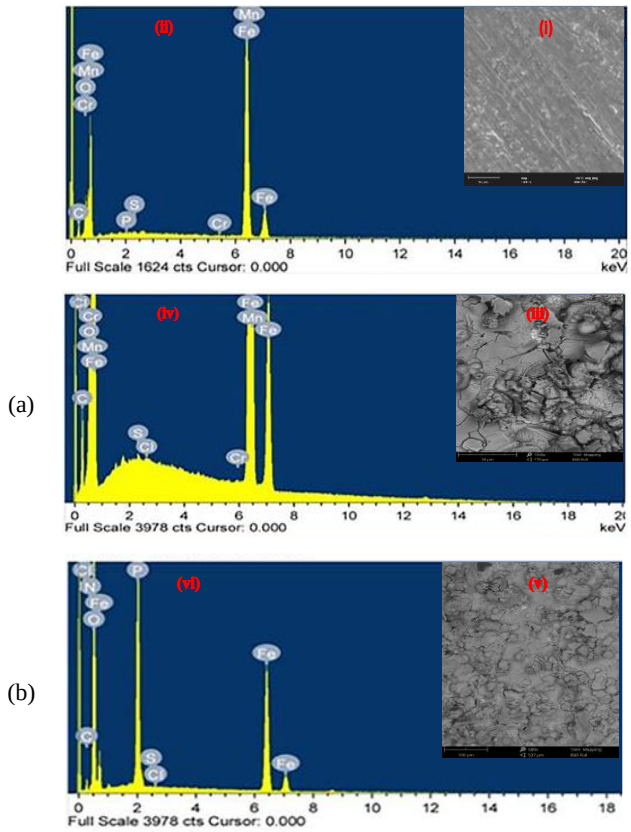

Fig. 7. (a) SEM micrographs (i) with the corresponding EDX Spectrum (ii), for polished X120 steel (b) SEM micrographs (iii) with the corresponding EDX Spectrum (iv), for X120 steel in free 15% HCl (c) SEM micrographs (v) with the corresponding EDX Spectrum (vi), for X120 steel in 15% HCl + 400 ppm DD.

The elemental composition of the X120 steel surface before and after exposure to the 15% HCl solutions without and with 400 ppm DD was determine by the EDX spectra and the atomic weight percentages tabulated in Table 4. The results of polished X120 steel specimen, before immersion into the corrosive medium, as seen in **Fig. 7a(ii)** contain little quantity of C, O, P, S, Cr, Mn and mostly Fe but without chlorine. Nonetheless, the EDX spectrum of the X120 steel specimen in 15% HCl solution without inhibitor showed reasonable amount of chlorine on the surface of steel due to the adsorbed chloride ions on

the steel surface [**43**]. In the presence of DD, the EDX spectra showed increased peaks oxygen atom and peaks of nitrogen atom. This is due to the presence of O and N atoms in the DD inhibitor molecule which is adsorbed on the X120 steel surface. Likewise, the peak of carbon is reasonable increased due to the presence of carbon atoms in the adsorbed inhibitor molecule.

Table 5. Weight percentage elemental contents obtained from EDX spectra of X120 steel in the absence and presence of inhibitors in 15% HCl.

Medium	Elemental composition								
	Fe (%)	Mn (%)	O (%)	Cr (%)	C (%)	P (%)	S (%)	Cl (%)	N (%)
Polished X120 steel	98.09	0.61	0.05	0.68	0.44	0.05	0.08	-	-
15% HCl	83.95	0.36	6.87	0.25	1.51	-	0.09	6.97	-
15% HCl + 400 ppm DD	86.39	-	4.96	-	7.53	0.04	0.06	0.83	0.19

Conclusion

The results obtained from electrochemical (EIS and PDP) and gravimetric methods showed that the studied drug exhibits good protection ability towards X120 steel corrosion in acidic 15% HCl solution and their inhibition performance increases with increase in DD concentration. Polarization study revealed that DD behaved as mixed type inhibitor. EIS measurements showed that DD inhibits corrosion by forming a protective film on the X120 steel surface thereby reducing the charge transfer rate. The adsorption of the inhibitor on the metal surface obeyed the Langmuir isotherm. SEM-EDX analyses show that X120 steel surface is protected in presence of DD which supports the adsorption mechanism of the inhibitor.

Acknowledgements

Lebe A. Nnanna and Nkem B. Iroha gratefully acknowledge Michael Okpara University of Agriculture, Umudike, Nigeria for the financial support and facilitation of study.

Keywords

Diphenoxylate, API X120 steel, corrosion inhibition, surface morphology, langmuir isotherm.

Received: 31 January 2020
Revised: 26 February 2020
Accepted: 27 February 2020

References

1. El-Maksoud, S. A. A.; Fouda A. S.; *Mater. Chem. Phys.*, **2005**, 93, 84.
2. Keles H.; Keles M.; Dehri I.; Serindag O.; *Mater. Chem. Phys.*, **2008**, 112, 173.
3. Crowe, C.; Masmonteil, J.; Thomas, R.; *Oilfield Rev.*, **1992**, 4, 22.
4. Giacomelli, F.C.; Giacomelli. C. *Giacomelli. Mater. Chem. Phys.* **2004**, 83, 124
5. Moretti, G.; Guidi, F.; *Corros. Sci*. **2004**, 46, 387.
6. Ahmed, S. K.; Ali, W. B.; Khadom, A. A., *Int J Ind Chem*., **2019**, 10, 159
7. Ahmed, S.K., Ali, W.B.; Khadom, A.A. *J. Bio Tribo Corros*, **2019**, 5, 15.
8. Kosec, T.; Milošev I.; Pihlar, B.; *Appl. Surf. Sci*., **2007**.253, 8863.
9. Iroha, N. B.; James, A.O. *WNOFNS*.; **2019**, *27*, 22.
10. Obot, I. B.; Obi-Egbedi, N. O.; Umoren, S. A. *Corros Sci.*, **2009**, *51* 8, 1868.
11. Nouri, P. M.; Attar, M. M.; *Bull. Mater. Sci.*, **2015**, *38*, 499.
12. Iroha, N.B.; Nnanna, L.A.; *J. Mater. Environ. Sci*., **2019**, *10*, 898.
13. Mohana, K. N.; Bediea, A. M.; *Corros. Sci.*, **2008**, *50*, 2939.
14. Iroha, N. B.; Madueke, N. A.; *Chemical Sci. Inter. J*. **2018**, 25, 1
15. Thirumoolan, D.; Katkar, V. A.; Gunasekaran, G.; Kanai, T.; Basha, K. A.; *Prog. Org. Coat.*, **2014**, *77*, 1253.
16. Mobin, M.; Khan, M. A.; *Chem. Eng. Commun*., **2013**, *200*, 1149.
17. James, A. O.; Iroha, N. B.; *IOSR J. Appl. Chem*., **2019**, *12*, 1.
18. El-Taib Heakal, F.; Deyab, M. A.; Osman, M. M., Elkholy, A. E., *Desalination*, **2018**, *425*, 111.
19. Iroha, N. B.; Hamilton-Amachree, A.; *World Scientific News*, **2019**. *126*, 183.
20. Roy, P.; Pal, A.; Sukul, D.; *RSC Adv*., **2014**, *4*, 10607.
21. Lozano, I.; Mazario, E.; Olivares-Xometi, C. O.; Likhanova, N. V.; Herrasti, P.; *Mater. Chem. Phys.*, **2014**, *147*, 191.
22. Ibrahim, M. A.; Messali, M.; Moussa, Z.; Alzahrani, A. Y; Alamry, S. N; Ham-mouti, B.; *Portugaliae Electrochim Acta*, **2011**, *29*, 375.
23. Martinez, S.; Metikos-Hukovic, M. A.; *J. Appl. Electrochem.*, **2003**, *33*, 1137.
24. Haque, J.; Srivastava, V.; Verma, C.; Quraishi, M. A.; *J. Mol. Liq.*, **2017**, *225*, 848.
25. Iroha, N. B.; Chidiebere, M. A.; *Inter. J. Mater. Chem*., **2017**, *7*, 47.
26. Ferreira, E. S.; Giancomelli, C.; Giacomelli, F.C.; Spinelli, A.; **2004**, *Mater. Chem. Phys., 83*, 129.
27. Noyel Victoria, S.; Prasad, R.; Manivannan, R.; *Int. J. Electrochem. Sci.*, **2015**, *10*, 2220.
28. Chidiebere, M. A.; Simeon, N.; Njoku, D.; Iroha, N. B.; Oguzie, E. E.; Li, Y.; **2017**, *WNOFNS*, *15*, 1.
29. John, S.; Joseph, A.; *Mater. Chem. Phys.*, **2012**, *133*, 1083.
30. Singh, A. K.; Quraishi, M. A.; *Corros. Sci*., **2009**, *51*, 2752.
31. Umoren, S. A.; Li, Y.; Wang, F. H.; *Corros. Sci*., **2010**, *52*, 1777.
32. Labjar, N.; Lebrini, M.; Bentiss, F.; Chihib, N. E.; El Hajjaji, S.; Jama, C.; *Chem. Phys.*, **2010**, *119*, 330.
33. Roy P, Sukul D.; *RSC Adv*. **2015**, *5*, 1359.
34. Hamilton-Amachree, A.; Iroha, N. B.; *Chem. Inter*., **2020**, 6(3), 117.
35. Gholami, M.; Danaee, I.; Maddahy, M. H.; RashyandAvei, M.; *Ind.Eng. Chem. Res.* **2013**, *52*, 14875.
36. Jeyaprabha, C.; Sathiyanarayanan, S.; Venkatachari, G.; *Electrochim. Acta*. **2006**, *51*, 4080.
37. Rokovic, M. K.; Kvastek, K.; Horvat-Radosevic, V.; Duic, L. *Corros. Sci*. **2007**, *49*, 2567.
38. Li, Y.; Zhang, S.; Dinga, Q., Qin, B.; Hu..; L.; *J. Mol. Liq.*, **2019,** *284*, 577.
39. Jacob, K. S.; Parameswaran, G.; *Corros Sci*., **2010**, *52*, 224.
40. Yoo, S. H., Kim, Y. W., Chung, K.; Kim, N. K.; Kim, J. S.; *Ind Eng Chem Res*.; **2013**, *52*, 10880.
41. Yadav, M.; Behera, D.; Kumar, S.; Sinha, R. R.; *Ind Eng Chem Res* **2013**, *52*, 6318.
42. Jafari, H.; Danaee, I.; Eskandari, H.; Rashvandavei, M.; *Ind Eng Chem Res*, **2013**, *52*, 6617.
43. Ramaganthan, B.; Gopiraman, M.; Olasunkanmi, L. O.; Kabanda, M. M.; Yesudass, S.; Bahadur, I.; Adekunle, A. S.; Obot, I. B.; Ebenso, E. E.; *RSC Adv*., **2015**, *5*, 76675.